Barrier Properties of Titanium Nitride Films Grown by Low Temperature Chemical Vapor Deposition from Titanium Tetraiodide

Cheryl Faltermeier, Cindy Goldberg, Michael Jones, Allan Upham, Dirk Manger, Gregory Peterson, Janice Lau, and Alain E. Kaloyeros

New York State Center for Advanced Thin Film Technology and Department of Physics, The University at Albany, State University of New York, Albany, New York 12222, USA

Barry Arkles

Gelest, Incorporated, Tullytown, Pennsylvania 19007, USA

Ajit Paranjpe[a]

Texas Instruments, Incorporated, Dallas, Texas 75265, USA

ABSTRACT

Results are presented from a systematic study of the composition, texture, and electrical properties of titanium nitride (TiN) films and their performance as diffusion barrier in multilevel interconnect schemes of ultralarge scale integration (ULSI) computer chip device structures. The films were grown by low temperature (<450°C) inorganic chemical vapor deposition using titanium tetraiodide as source precursor and ammonia and hydrogen as co-reactants. The TiN films were nitrogen-rich., with iodine concentrations below 2 atom percent, displayed resistivities in the range 100 to 150 $\mu\Omega$ cm depending on thickness, and exhibited excellent step coverage with better than 90% conformality in both nominal 0.45 μm, 3:1 aspect ratio and 0.25 μm, 4:1 aspect ratio contact structures. A comparison of the properties of chemical vapor deposited (CVD) TiN with equivalent physical vapor deposited (PVD) TiN showed that reactivity with Al-0.5 a/o Cu alloys was equivalent in both cases. In particular, a 10% increase in the Al-Cu/TiN stack sheet resistance was observed for both types of TiN after a 450°C, 30 min sinter. Similarly, the characteristics of CVD tungsten and reflow plug fills were identical on both types of TiN films. However, barrier performance for CVD TiN in aluminum and tungsten plug technologies was superior to that of PVD TiN, as evidenced by lower contact diode leakage for CVD TiN in comparison with PVD TiN films of equal thickness. This improved barrier performance could be attributed to a combination of factors, which include the nitrogen-rich composition, higher density, and enhanced conformality of the CVD TiN phase in comparison with the PVD TiN. In view of the superior step coverage and diffusion barrier characteristics, the low temperature inorganic CVD route to TiN seems to provide an adequate replacement for conventional PVD TiN in emerging ULSI metallization interconnect schemes.

Introduction

Titanium nitride (TiN) is a commonly used material in current integrated circuit (IC) technologies.[1] Its applications range from diffusion barrier and glue layer at the contact/via level to diffusion barrier and antireflection coating in the interconnect stack.[2] Such applications are made possible by the desirable properties of TiN, including its refractory nature at elevated temperature, excellent mechanical, chemical, and thermal inertness, and good resistance to corrosion. These properties allow TiN to withstand the repeated thermal cycles use in multilevel metallization of IC devices, and make its continued use in emerging subquarter micron device technologies highly desirable. However, the suitability of TiN for such applications is only possible if it is deposited with good conformality in subquarter micron features, leading to void-free plug formation, reduced junction leakage, and low contact/via resistance. This requirement is further complicated by a strong push to reduce barrier thickness, as device size shrinks, to provide the cross section of aluminum or copper conductor required for optimum device performance.

Conventional physical vapor deposition (PVD) routes to TiN, with their inherent line of sight type deposition, appear to have reached their maximum useful lifetime, even with the addition of special features such as collimators.[3] Modified PVD processes, including high density plasma sputtering, appear to provide acceptable near term solutions, at least for the 0.25 μm device generation.[4-6] Chemical vapor deposition (CVD), on the other hand, offers a low temperature alternative which is inherently capable of conformal metal growth. By combining simplicity, controllability, and ability to coat large area substrates with excellent uniformity at industrially viable growth rates, CVD could potentially meet performance demands well into the 0.18 μm device technology and beyond.

Early attempts at preparing CVD TiN used mostly titanium tetrachloride ($TiCl_4$) and ammonia (NH_3) to yield stoichiometric TiN films having good step coverage.[7] The impurities produced by this process, mainly chlorine, were within 1 atomic percent (a/o). Unfortunately, the processing temperatures required to produce these films were in excess of 650°C, and were thus prohibitive for use above the contact level. Efforts to reduce deposition temperatures included plasma-assisted CVD (PACVD) of $TiCl_4$ in a mixture of nitrogen and hydrogen, electron cyclotron resonance (ECR) plasma CVD of $TiCl_4$ in a nitrogen atmosphere,[8] and atmospheric pressure CVD (APCVD) using $TiCl_4$ and isopropylamine or tert-butylamine as the coreactant.[9] These efforts led to an appreciable reduction in process temperatures to within the acceptable range of about 350 to 500°C. However, various reliability issues ranging from poor step coverage (30 to 70%) in some cases, to high resistivities (> 200 $\mu\Omega$ cm) and chlorine contamination above several atomic percent, in other cases, prevented their incorporation in the IC process flow.

There are several recent reports on metallorganic CVD (MOCVD) of TiN from dialkylamino derivatives of titanium of the type $Ti(NR_2)_4$, where R is a methyl or ethyl group.[10] Additional MOCVD studies involved the use of single-source titanium precursors of the type $[TiCl_2(NHR_2)(NH_2R)_{n-2}]$ and $[TiCl_4(NR_3)_2]$, and cyclopentadienyl-based titanium compounds of the type biscyclopentadienyl titanium diazide, $Cp_2Ti(N_3)_2$ (where Cp = C_5H_5).[11] These activities led to the development of robust and ver-

[a] Present address: CVC Products, Inc., Rochester, New York 14603, USA.

satile MOCVD TiN processes,[12] with MOCVD from $Ti(NEt_2)_4$, for example, yielding resistivity below 300 μΩ cm, carbon contamination under 3 a/o, and step coverage as high as 70% in 0.35 μm device structures.

The strategy espoused herein has focused, instead, on low temperature inorganic CVD of TiN from titanium tetraiodide (TiI_4). TiI_4 was selected because the dissociation energy of the Ti-I is relatively low, with a corresponding heat of formation at 298 K of −92 kcal/mol. This value is well below the heat of formation for $TiCl_4$, namely, −192 kcal/mol. Accordingly, and in view of the similar chemical characteristics of the two halide chemistries, TiI_4 is expected to yield TiN films in an ammonia atmosphere with properties and performance similar to those from $TiCl_4$ but at significantly lower temperature.

Additionally, the activation energy for iodine diffusion is expected to be significantly higher than chlorine, given that I is a much heavier element than Cl. This expectation is based on work on the interaction of fluorine and chlorine with (111) Si,[13] and which showed that the barrier for chlorine penetration into the Si surface is much larger than that for fluorine. This behavior was a consequence of the larger size, and hence ionicity and resulting coulomb interaction, of the chlorine atom in comparison with fluorine. This property has important implications for the effects of residual halide incorporation in the deposited TiN, with 1 a/o iodine requiring appreciably higher thermal energy to diffuse out of TiN lattice than its chlorine counterpart. This observation is also supported by the findings presented herein, including diode leakage measurements, and which indicate that 2 a/o iodine did not affect TiN performance as diffusion barrier/adhesion promoter.

The paper is the second in a series of reports on the identification and optimization of a low temperature inorganic CVD process for TiN from TiI_4.[14] The first report has focused on the development of a low-temperature, *in situ*, sequential CVD process for the deposition of ultrathin Ti/TiN bilayers for applications in device ULSI technologies. In this article, results are presented from a systematic study of the microstructural, microchemical, and electrical characteristics of TiN films, as well as their performance in 0.45 μm, 3:1 aspect ratio contact/plug device structures. The findings from this study are compared and contrasted with those from PVD TiN grown by conventional PVD techniques.

Experimental

The CVD reactor used for inorganic CVD of TiN from TiI_4 was a custom-made, 8 in. wafer, cold wall system, and was described in detail elsewhere.[13] Briefly, it consisted of a parallel plate plasma configuration with the wafer located on the bottom electrode, which was resistively heated using an externally positioned boron nitride-coated graphite heater. The top active electrode was formed in the shape of a circular mesh to allow unrestricted flow of the reactants through a cone-shaped shower head located above the mesh. Pumping was achieved through eight ports which were symmetrically distributed below the heater chuck to permit uniform gas flow distribution. A standard pressure based sublimator was used to store the solid TiI_4 precursor, which was delivered to the reaction zone with the assistance of a hydrogen carrier gas. Ammonia reactant flow was delivered through a sideline directly to the reaction zone. A soft hydrogen plasma predeposition clean was performed on all samples prior to deposition. However, no plasma was used during actual deposition. Several types of wafers were processed, as shown in Table I, using the process conditions summarized in Table II.

Methods of Analysis

The TiN film microchemical, microstructural, and electrical properties were thoroughly analyzed at the New York State Center for Advanced Thin Film Technology by x-ray photoelectron spectroscopy (XPS), Rutherford backscattering (RBS), x-ray diffraction (XRD), four-point resistivity probe, and cross-sectional scanning electron microscopy (CS-SEM). In these studies, the results were standardized using a pure TiN standard deposited by collimated sputtering at SEMATECH. Additional compositional and structural characterization was also carried out independently at SEMATECH.

Film composition was determined using XPS and RBS. XPS was carried out on a Perkin-Elmer PHI 5500 Multi-Technique System. A magnesium x-ray source at 15 kV and 300 W was used. High resolution XPS scans employed a 23.50 eV pass energy to resolve shifts from particular photoelectron peaks.

In addition to performing compositional characterization, RBS was also employed, in conjunction with CS-SEM, for thickness and growth rate measurements. Rutherford backscattering (RBS) spectra were taken using a 2 MeV He^+ beam, and calibrated with bulk samples of gold and carbon, while CS-SEM investigations employed a Zeiss DSM 940 microscope using a 20 keV primary electron beam. Four-point probe resistivity measurements used a Signatone four-point probe. Deposition rates were defined as T/t, where T is film thickness and t is run time. Run time was measured starting form the instant when the precursor was actually being delivered to the reactor.

X-ray diffraction was done on a Scintag XDS 2000 x-ray diffractometer. X-rays were generated with a Cu K_α x-ray source at typical tube operating power of 1.8 kW, which corresponds to 40 mA and 45 kV. XRD spectra were collected both in normal incidence and 5° grazing angle geometries. The resulting TiN XRD patterns were compared with the sputtered TiN standard provided by SEMATECH and a TiN reference pattern from the standard JCPDS powder diffraction file (PDF).

A complete evaluation of the physical properties and barrier characteristics of the TiN films was carried out at the Semiconductor Process and Device Center of Texas Instruments. The microchemical and electrical measurements performed above at the Albany Center were repeated as an independent checking mechanism of TiN film properties. The parameters measured and corresponding methods of analysis are summarized in Table III and discussed in more detail in the following sections. In these studies, the results were standardized using a pure TiN standard deposited by collimated sputtering at Texas Instruments.

Table I. Type and number of wafers used in the study.

Wafer type	Number of wafers	Thickness CVD TiN
1000 Å PETEOS/Si	2	900 ± 50 Å
Si	2	30 ± 2 Å
Si	2	230 ± 5 Å
0.45 μm contact	3	620 ± 12 Å
0.45 μm contact	2	230 ± 5 Å
0.45 μm contact	1	300 ± 10 Å
0.45 μm contact	1	400 ± 10 Å
0.45 μm contact/n^+ salicide junction	3	30 ± 2 Å
0.45 μm contact/n^+ salicide junction	3	230 ± 5 Å
0.45 μm contact/n^+ salicide junction	3	400 ± 10 Å

Table II. Summary of processing parameters.

Process parameter	Value
Source precursor	TiI_4
Wafer temperature	430°C
Source temperature	140°C
Reactor pressure	0.3 torr
Ammonia reactant flow	600 sccm
Hydrogen carrier gas flow	30 sccm
In situ predeposition Hydrogen Plasma clean	13.56 Mhz@ 0.08 W/cm^2

Table III. Methods of analysis.

Parameter	Method
Sheet resistance	Four-point probe (900 Å TiN on 1000 Å PETEOS/Si)
Thickness	Profilometry (900 Å TiN on 1000 Å PETEOS/Si) RBS
Density	Weight gain (900 Å TiN on 1000 Å PETEOS/Si)
Composition	RBS and XPS (900 Å TiN on 1000 Å PETEOS/Si)
Step coverage	CS-SEM (230, 400, 900 Å TiN on 0.45 and 0.25 μm contact)
Barrier attack	230, 400, 600 Å TiN on 0.45 μm contact
Barrier properties	Used 30 to 230 Å CVD TiN on Si: (*i*) Deposited 600 Å Al-0.5 a/o Cu then sintered at 450 to 550°C for 30 to 60 min. (*ii*) Measured pre- and post Al-Cu sheet resistance. (*iii*) After sintering, metal was stripped and optical microscopy used to quantify pit density in Si. (*iv*) Samples on Si, plasma TEOS, PVD TiN were similarly processed and used for comparison.
W plug fill	CS-SEM (230, 400, 900 Å TiN on 0.45 μm contact
Contact resistance	30 to 400 Å TiN on 0.45 μm contact/n^+ salicide junction
Diode leakage	30 to 400 Å TiN on 0.45 μm contact/n^+ salicide junction

The 900 Å CVD TiN films on plasma tetraethylorthosilicate (PETEOS) were analyzed for sheet resistance, sheet resistance uniformity, thickness, density and composition/stoichiometry. Sheet resistance was measured using a four-point probe, thickness was calculated using a profilometer, density was determined from weight gain measurements, and composition/stoichiometry was determined from RBS analysis. For the RBS analysis, a PVD (conventional sputtering) TiN film was used as control for comparison.

The 30 to 230 Å CVD TiN films on Si were used for barrier studies. A 6000 Å Al-0.5 a/o Cu film was sputter deposited on the CVD TiN and the stack was subjected to sintering at 450 to 550°C for 30 to 60 min. Sheet resistance measurements prior to and after sintering were used to quantify the reaction between Al-Cu and CVD TiN. After sintering was complete, the metal was stripped and the density of pits in the silicon was measured on an optical microscope to quantify the quality of the CVD TiN barrier. 6000 Å Al-0.5 a/o Cu films deposited directly on Si, plasma TEOS, and PVD TiN were also subjected to similar sinter cycles for comparison. The patterned contact wafers were used for step coverage measurements and to evaluate nucleation, barrier attack, and plug-fill during CVD tungsten deposition. Finally, the contacts on the n^+ salicided junctions were used to measure contact resistance and contact-induced diode leakage.

Results

The TiN films thus produced were metallic, mirror-like, and gold colored. Their physical properties are summarized in Table IV and discussed in more detail below. In particular, deposition nonuniformity is slightly high, but is an equipment not a process issue, given that a custom-made, nonoptimum, reactor was used in the study.

Film composition.—The composition of the films was examined by XPS and RBS. XPS depth profiling, as shown in Fig. 1, indicated a nitrogen-rich $TiN_{1.06}$ phase with iodine concentration below 2 a/o. No oxygen or other contaminants were found within the detection limits of XPS (~1a/o). Additionally, XPS high resolution spectra of elemental core levels yielded a Ti $2p_{3/2}$ core peak at 455.1 eV, as displayed in Fig. 2, corresponding to a pure TiN phase. Figure 3 shows the N 1s binding energy at 397.3 eV, also indicating a pure TiN phase.

Table IV. Summary of results.

Parameter	Value
Deposition rate (Å/min)	200
Nonuniformity (%, 1σ)	5 to 8
Step coverage (%)	90
Resistivity (μΩ cm)	100 to 150
Stoichiometry (Ti:N)	1:1.06
Impurities	<2 a/o iodine <1 a/o oxygen
Density	1.1 times that of PVD TiN
Color	Golden
Stability (ΔR_s/2 h, %)	Zero
CVD W plug fill	Similar to PVD TiN
Al reflow plug fill	Similar to PVD TiN
Reactivity with Al-Cu	Similar to PVD TiN
Barrier property	Superior to PVD TiN

RBS analysis of TiN on Si also supported the XPS results, and indicated the presence of about 2 a/o iodine incorporation, as displayed in Fig. 4.

The composition of the CVD produced TiN films was nitrogen-rich in comparison with the SEMATECH collimated PVD TiN. Levels of iodine in the films are not

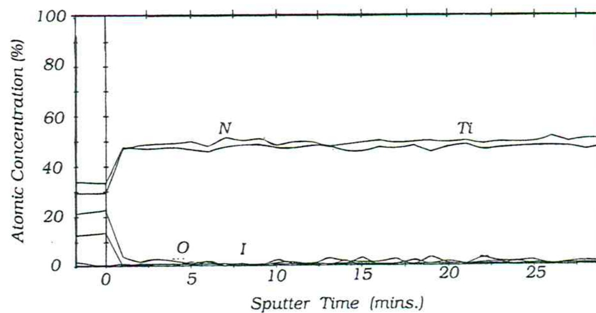

Fig. 1. XPS depth profiling indicates a stoichiometric TiN phase with iodine concentration below 2 a/o. No oxygen or other contaminants were found within the detection limits of XPS.

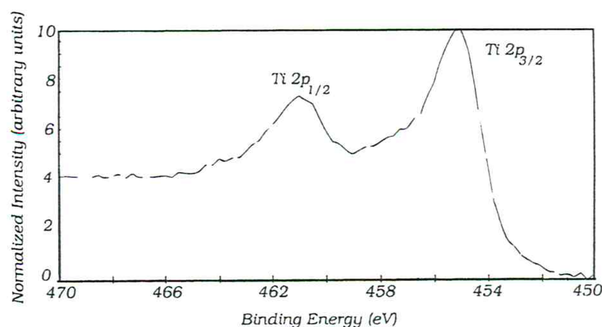

Fig. 2. XPS high resolution spectrum of Ti $2p_{3/2}$ indicates a core peak at 455.1 eV corresponding to a pure TiN phase.

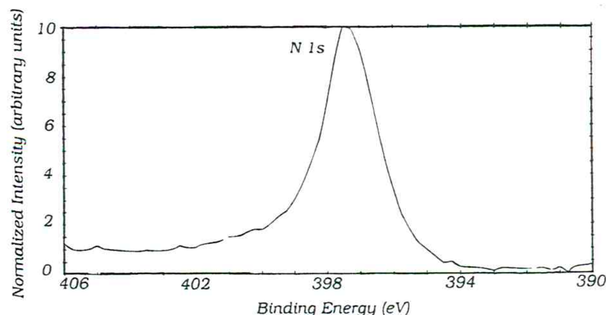

Fig. 3. The XPS N 1s binding energy at 397.3 eV indicates a pure TiN phase.

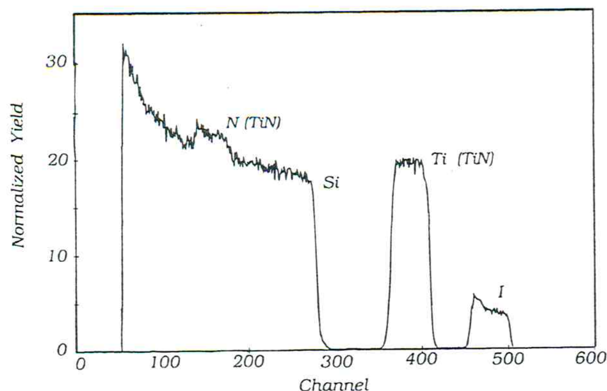

Fig. 4. RBS analysis of TiN on Si supports the XPS results, and indicates the incorporation of about 2 a/o iodine.

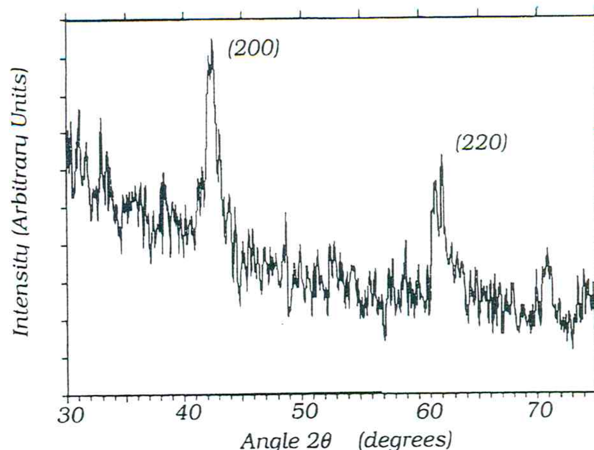

Fig. 6. XRD spectrum of a sputter-deposited TiN film.

expected to pose any reliability problems, such as Si wormhole formation and metal corrosion. This assessment is attributed to the higher activation energy for iodine diffusion as compared with chlorine, given that I is much heavier than Cl. Accordingly, it is expected that 1 a/o iodine might require appreciably higher thermal energy to diffuse out of the TiN lattice than its chlorine counterpart, thus posing less of a reliability problem. This assumption is supported by the findings presented herein and which demonstrate that TiN barrier integrity and device performance are not compromised by 2 a/o residual iodine levels. It is also in agreement with similar work reported by Yokoyama *et al.* on the mobility of chlorine in CVD TiN produced from the reaction of $TiCl_4$ and NH_3.[15]

Film texture.—Figure 5 shows a typical XRD spectrum of a CVD TiN film. The spectrum exhibited reflections corresponding to $2\theta = 42.34°$ (111) and 61.98 (220), with the (111) orientation exhibiting the highest diffraction intensity. Interestingly, the XRD spectrum displayed in Fig. 6 from SEMATECH's sputter-deposited TiN film showed a different XRD texture, with the (200) orientation showing the strongest diffraction peak. Interestingly, Yokoyama *et al.* also observed textural variations between CVD and PVD TiN.[16]

The textural variations observed might have significant implications for the barrier characteristics and associated differences in the peformance of CVD and PVD grown films. Additionally, it has been shown that the texture of the TiN film can significantly affect that of the overlaying aluminum film. Primarily, predominantly (200) textures TiN leads to the formation of similarly textured aluminum, while (111) oriented TiN produces an identical aluminum orientation. This effect is important since predominantly (111) oriented aluminum exhibits enhanced electromigration resistance and increased mean time to failure (MTTF) under electromigration stress conditions in comparison with its (200) counterpart.[17] Additional studies are underway to study these effects and will be reported in a subsequent publication.

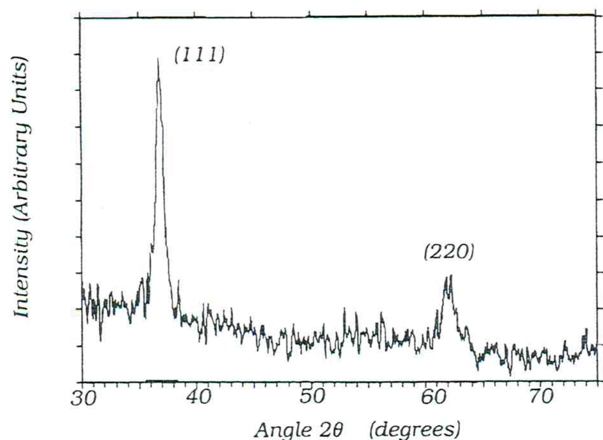

Fig. 5. Typical XRD spectrum of a CVD TiN film. The diffraction peak locations and intensities are in good agreement with those from a standard TiN powder sample, indicating that the TiN film is polycrystalline.

Aggressive structure fill and resistivity.—Figure 7 displays typical CS-SEM micrographs of TiN step coverage in aggressive device trench structures, with nominal feature size of 0.45 μm, 3:1 aspect ratio. As can be seen, step coverage is excellent, with 90% conformality observed in the structures examined. Interestingly, highly conformal TiN coverage was achieved across a wide process window, as demonstrated in Fig. 8 which shows 90% TiN step coverage in 0.25 μm, 4:1 aspect ratio structures. These samples were processed at a substrate temperature of 425°C, source temperature of 140°C, reactor pressure of 0.5 Torr, and hydrogen carrier gas and ammonia reactant flows of, respectively, 30 and 400 sccm. The values observed are significantly higher than those that can be obtained using collimated PVD TiN. Film resistivity ranged from 100 μΩ cm for 1000 Å films up to 150 μΩ cm for 100 Å films.

Barrier properties.—The density of the film is high, 1.1 times that of the collimated PVD TiN as tested by Texas Instruments, and the films have a strong golden color. Films are stable in air and showed no evidence of oxidation, even after prolonged exposure to air. Plug filling with CVD tungsten and Al reflow are similar for vias lined with CVD TiN or PVD TiN. Reactivity with Al-0.5% Cu during a 450°C, 30 min forming gas sinter was similar to the reactivity of PVD TiN. The sheet resistance increase upon sintering is marginally lower for CVD TiN compared to PVD TiN, as observed in Fig. 9. The various splits indicate that the sheet resistance increase is due to interaction between the Al-Cu and TiN rather than between Al-Cu and Si. After a 550°C, 60 min sinter, splits 1, 2, and 4 show pitting of the Si surface indicative of barrier failure. However the density of pits is maximum for the case of no barrier, and is minimum for the CVD TiN barrier.

Superiority of the CVD TiN barrier can also be gauged from the contact-induced diode leakage for a diode with 250,000 contacts (Fig. 10). The diode leakage characteristics for a 230 Å CVD TiN film are equivalent to those for a 500 Å PVD TiN film. Increasing the CVD TiN thickness to 400 Å decreases the leakage further. There is no appreciable difference in diode leakage for block diodes with few contacts except for the case of 30 Å CVD TiN which appears to be too thin, or possibly not even continuous, to yield a reliable measurement (Fig. 11). Additionally, the wider dispersion in the diode leakage current for the 400 Å TiN film is attributed to a larger than typical thickness

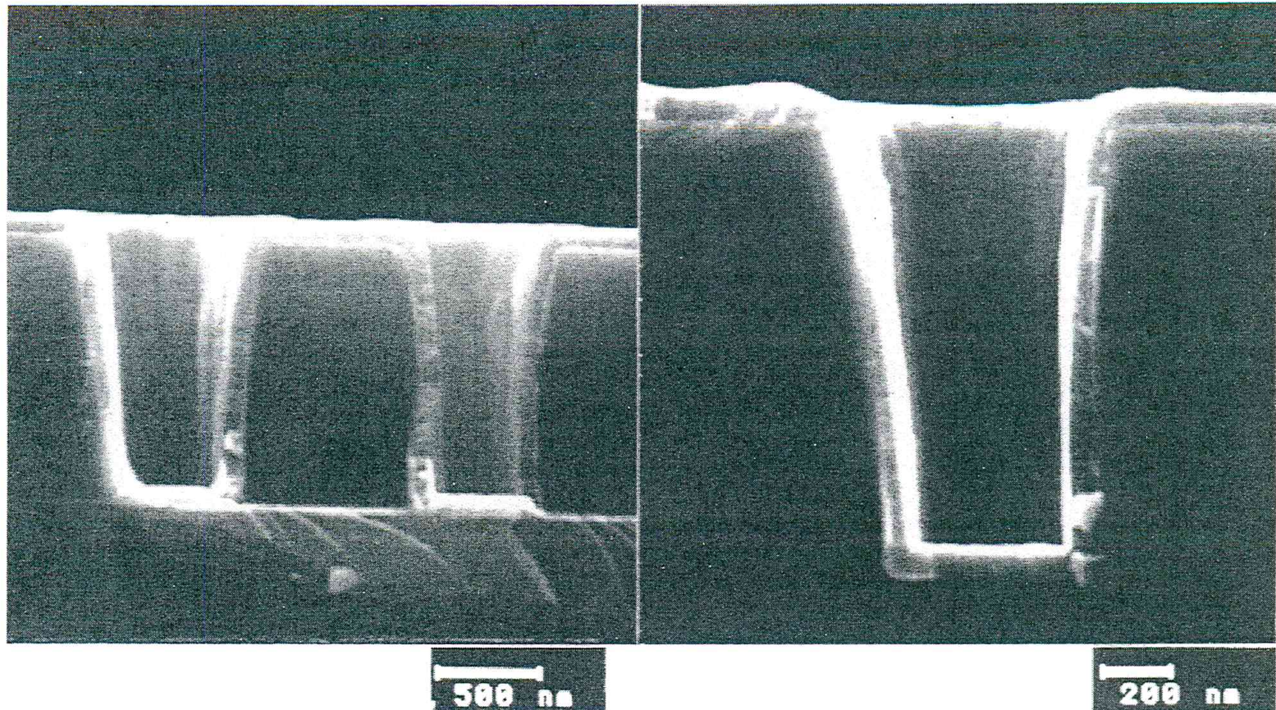

Fig. 7. Typical CS-SEM micrograph of TiN step coverage in 0.45 μm, 3:1 aspect ratio contacts.

variation across the specific wafer used in those measurements. Accordingly, the worst leakage value corresponded to a spot on the wafer where the TiN was thinner than 400 Å.

Discussion and Conclusions

The results discussed above demonstrate that the low temperature inorganic CVD route is a viable approach for the deposition of TiN for applications as barrier layer and adhesion promoter in emerging subquarter micron device technologies. The TiN films thus produced were gold colored, stoichiometric, and exhibited metallic conductivity, with resistivities in the range of 100 to 150 μΩ cm, depending on film thickness. Microchemical analyses showed that the films were free from oxygen or carbon contamination, within the detection limits of XPS, with iodine concentrations below 2 a/o. Such levels of iodine concentrations are not expected to cause reliability problems in device operation. This expectation is based on the assumption that iodine is significantly heavier than chlorine and will thus require higher activation energy for diffusion out of the TiN matrix. The diode leakage data presented herein seems to also support this assessment.

A systematic evaluation was also carried out of the barrier characteristics of CVD TiN using PVD TiN as base line material. The data showed that reactivity with Al-0.5 a/o Cu alloys was equivalent in both cases, with the CVD TiN film exhibiting a marginally better performance as compared to its PVD counterpart. Similarly, the characteristics of CVD tungsten and reflow plug fills were identical on both types of TiN films. However, barrier performance

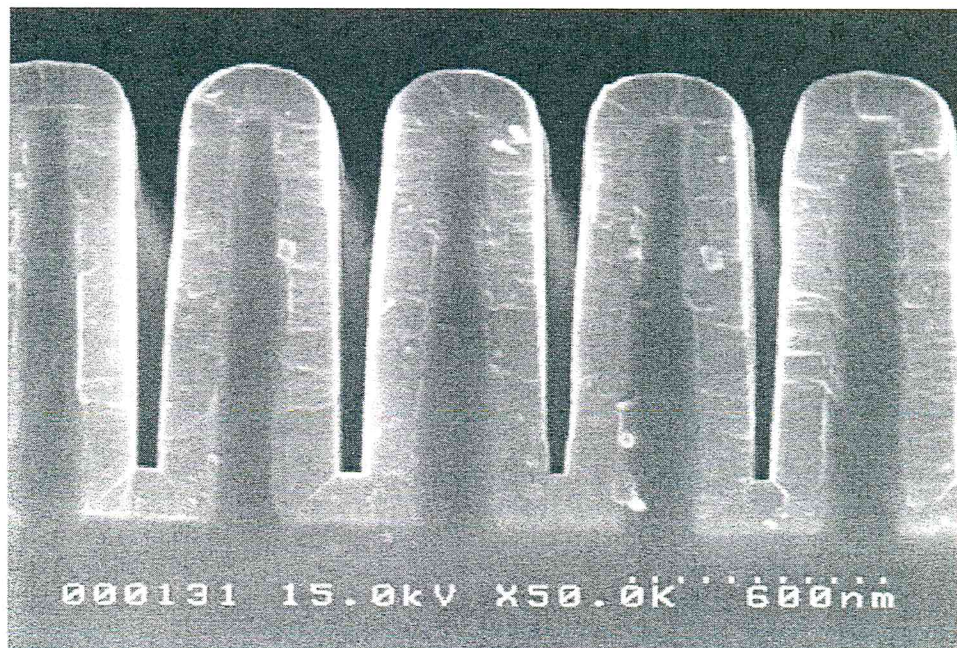

Fig. 8. Typical CS-SEM micrograph of TiN step coverage in 0.25 μm, 4:1 aspect ratio contacts.

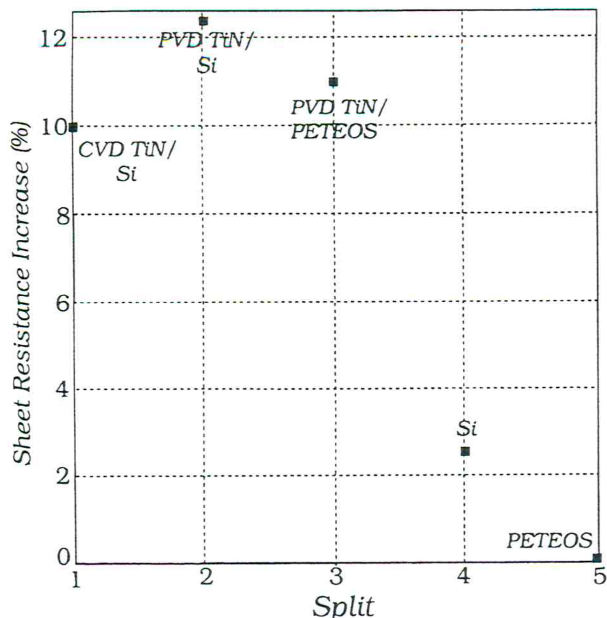

Fig. 9. Increase in sheet resistance of an Al-0.5%Cu/TiN stack after a 450°C, 30 min, forming gas sinter. Splits are: CVD TiN/Si, PVD TiN/Si, PVD TiN/PETEOS, Si, and PETEOS.

for CVD TiN in aluminum and tungsten plug technologies was superior to that of its physical vapor deposited (PVD) counterpart, as evidenced by lower contact diode leakage for CVD TiN in comparison with PVD TiN films of equal thickness.

This improved barrier performance could be attributed to a combination of factors, which include the nitrogen-rich composition, higher density, and enhanced conformality of the CVD TiN phase in comparison with the PVD TiN. Interestingly, the texture of the CVD TiN films exhibited marked differences from that of PVD TiN. Primarily, the CVD TiN XRD spectra showed a dominant contribution from the (111) orientation, while PVD TiN had the strongest peak intensity from the (200) orientation. This textural difference might possibly result in barrier performance variations between the CVD and PVD grown films, and will be thoroughly examined in a follow-up study.

Finally, the CVD TiN films demonstrated excellent step coverage, with better than 90% conformality in both nominal 0.45 μm, 3:1 aspect ratio and 0.25 μm, 4:1 aspect ratio contact structures. In view of this superior step coverage and diffusion barrier characteristics, the low temperature inorganic CVD route to TiN seems to provide an adequate replacement for conventional PVD TiN in emerging ULSI metallization interconnect schemes.

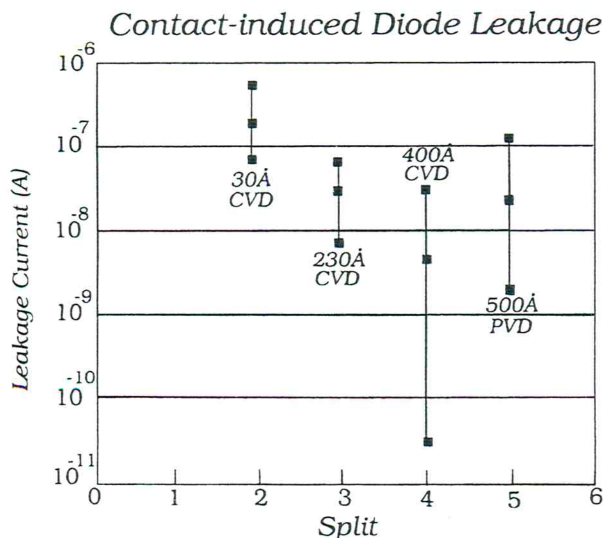

Fig. 10. Contact-induced diode leakage for contacts with 250,000 contacts. Splits are: 30 Å CVD TiN, 230 Å CVD TiN, 400 Å CVD TiN, and 500 Å PVD TiN. Symbols show quartile values.

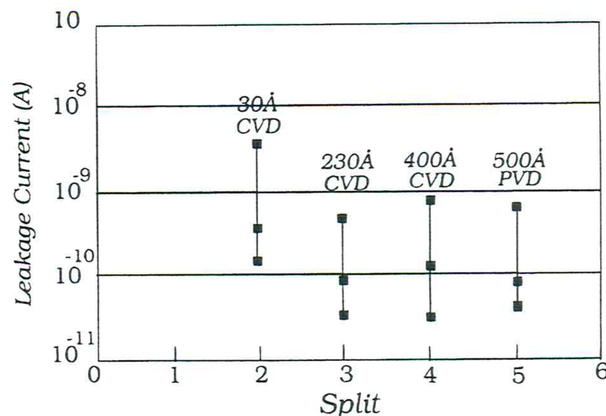

Fig. 11. Block diode leakage. Splits are: 30 Å CVD TiN, 230 Å CVD TiN, 400 Å CVD TiN, and 500 Å PVD TiN. Symbols show quartile values.

Acknowledgments

The work was supported by SEMATECH, under its J91 TiN Benchmarking Program, the New York State Center for Advanced Thin Film Technology (CAT), and the National Science Foundation (NSF) Presidential Young Investigator (PYI) award No. DMR-9157011. The authors thank Dr. Shi-Quing Wang (SEMATECH) for his valuable characterization work, and Dr. Mihal Gross (Lucent Technologies) for her helpful and insightful scientific discussions.

Manuscript submitted July 23, 1996; revised manuscript received Dec. 9, 1996.

The New York State Center for Advanced Thin Film Technology assisted in meeting the publication costs of this article.

REFERENCES

1. *The National Technology Roadmap for Semiconductors,* p. 94, Semiconductor Industry Association, San Jose, CA (1994).
2. S. P. Murarka, *Metallization: Theory and Practice for VLSI and ULSI,* Butterworth-Heinemann, Boston, MA (1993).
3. A. Intemann, H. Koerner, G. Ruhl, K. Hieber, and E. Hartmann, in *Advanced Metallization for ULSI Applications-X,* R. Blumenthal and G. Jenssen, Editors, p. 209, Materials Research Society, Pittsburgh, PA (1995).
4. J. M. Fu, M. Narasimhan, G. D. Yao, X. Xu, and F. Chen, in *Proceedings of the 12th International VLSI Multilevel Interconnection Conference,* p. 198, VMIC, Tampa, FL (1995).
5. A. Hobbs, K. Inoue, H. Takagi, K. Mashimo, T. Hosoda, and T. Nakamura, *ibid.,* p. 225.
6. I. Wagner, *ibid.,* p. 226.
7. See, for example, A. Sherman, *This Journal,* **137,** 1892 (1990); M. J. Buiting, A. F. Otterloo, and A. H. Montree, *ibid.,* **138,** 500 (1991); N. Yokoyama, K. Hinode, and Y. Homma, *ibid.,* **138,** 190 (1991).
8. See, for example, T. Akahori, and A. Tanihara, in *Proceedings of International Conference on Solid State Devices and Materials,* p. 180, Yokohama, Japan (1991); T. Miyamoto, A. Kawashima, S. Kadomura, and J. Aoyama, in *Proceedings of the 12th International VLSI Multilevel Interconnection Conference,* p. 195, VMIC, Tampa, FL (1995).
9. S. C. Selbrede, in *Advanced Metallization for ULSI Applications VIII,* T. S. Cale and F. S. Pintchovski,

Editors, p. 359, Materials Research Society, Pittsburgh, PA (1993).
10. See, for example: (a) R. M. Fix, R. G. Gordon, and D. M. Hoffman, *MRS Symp. Proc. Vol.*, **168**, 357 (1990); (b) K. Ishihara, Y. Yamazaki, H. Hamada, K. Kamisako, and Y. Tarui, *Jpn. J. Appl. Phys.*, **29**, 2103 (1990); (c) R. M. Fix, R. G. Gordon, and D. M. Hoffman, *Chem. Mater.*, **3**, 1138 (1991); (d) J. A. Prybyla and L. H. Dubois, in *Chemical Perspectives of Microelectronic Materials III*, C. R. Abernathy, C. W. Bates, Jr., D. A. Bohling, and W. S. Hobson, Editors, p 287, MRS, Pittsburgh, PA (1992).
11. C. H. Winter, T. Suren Lewkebandara, and P. H. Sheridan, *ibid.*, p. 293.
12. See, for instance, R. L. Jackson, E. J. McInerney, B. Roberts, J. Strupp, A. Velaga, S. Patel, and L. Halliday, in *Advanced Metallizatin for ULSI Applications-X*, R. Blumenthal and G. Jenssen, Editors, p. 223, Materials Research Society, Pittsburgh, PA (1995); G. A. Dixit, R. H. Havemann, L. Halliday, J. Strupp, B. Roberts, R. L. Jackson, and E. J. McInerney, in *Proceedings of 12th International VLSI Multilevel Interconnection Conference*, p. 175, VMIC, Tampa, FL (1995); G. A. Dixit, M. K. Jain, M. F. Chisholm, T. Weaver, R. H. Havemann, K. A. Littau, M. Eizenberg, S. Ghanayem, H. Tran, Y. Maeda, M. Chang, and A. Sinha, in *Advanced Metallization for ULSI Application X*, R. Blumenthal and G. Jenssen Editors, p. 239, Materials Research Society, Pittsburgh, PA (1995).
13. M. Seel and P. S. Bagus, *Phys. Rev. B*, **28**, 2023 (1983).
14. C. Goldberg, E. Eisenbraun, S. Komarov, C. Faltermeier, X. Chen, M. Jones, A. Ivanova, R. Fiordalice, F. Pintchovski, B. Arkles, A. Hepp, and A. E. Kaloyeros, in *Advanced Metallization for ULSI Application X*, R. Blumenthal and G. Janssen, Editors, p. 247, MRS Pittsburgh, PA (1995).
15. N. Yokoyama, K. Hinode, and Y. Homma, Abstract 466, p. 679 The Electrochemical Society Meeting Abstracts, Vol. 89-2, Hollywood, FL, Oct. 15-20, 1989.
16. N. Yokoyama, Y. Homma, and K. Mukai, U.S. Pat. 4,897,709 (1990).
17. B. Fiordalice, R. Hedge, and H. Kawasaki, *This Journal*, **143**, 2059 (1996).

Reprinted from JOURNAL OF THE ELECTROCHEMICAL SOCIETY
Vol. 144, No. 3, March 1997
Printed in U.S.A.
Copyright 1997